

We are IntechOpen, the world's leading publisher of Open Access books Built by scientists, for scientists

6,900

Open access books available

186,000

International authors and editors

200M

Downloads

Our authors are among the

154

Countries delivered to

TOP 1%

most cited scientists

12.2%

Contributors from top 500 universities



WEB OF SCIENCE™

Selection of our books indexed in the Book Citation Index
in Web of Science™ Core Collection (BKCI)

Interested in publishing with us?
Contact book.department@intechopen.com

Numbers displayed above are based on latest data collected.
For more information visit www.intechopen.com



Substituent Effect on Pyridine Efficacy as a Chelating Stabilizer

Amer A. G. Al Abdel Hamid

Additional information is available at the end of the chapter

<http://dx.doi.org/10.5772/intechopen.75046>

Abstract

Owing to the growing interest and unique properties of pyridines as bases, effects of substitution and substituent modification on electron density enrichment of the pyridyl nitrogen, and thus the effectiveness of pyridine as metal ion-stabilizers will be introduced in this chapter. Pyridines of the structure $C_5(S)nH_5-nN$ (S = substituent) that have been intensively studied theoretically were selected as examples to prove the concept of this chapter. Computational results in the reviewed reports showed that: substitution and substituent modification significantly affect the electronic enrichment of nitrogen atom of the pyridine. The conclusions extracted from the covered investigations were employed to promote pyridines to act as efficient stabilizers for the coordinated metal ions. In coordination chemistry, these kinds of coordinated complexes are highly demanded in the field of chemosensation.

Keywords: pyridine, chelating, substituent effect, DFT-calculation, electron density

1. Introduction

Pyridine is a six-membered N-heterocyclic molecule. It is characterized as relatively strong Brønsted basic [1, 2] and consequently its corresponding pyridinium salt as a relatively weak conjugate acid. Pyridine can serve as a solvent of high donor number [1, 3].

Pyridines compared to carbocyclic analogs have higher nitrogen contents and thus are capable of releasing sufficient delocalized electrons to the system they belong to, and therefore contribute more to the electron-donating activity in the parent compound than C-atom does in carbocyclic compounds. This is attributed to the fact that N-atom possesses a greater number of nonbonding valence electrons compared to C-atom. In effect, the inclusion of pyridine moiety into a molecule is assumed to enrich the molecule with electron density and, correspondingly, improves its stability and binding capability.

In result, and owing to their unique properties as bases, rather high electron density, high positive heat of formation, and good thermal stability [4–7] pyridines and related derivatives are efficiently utilized as chelates (*stabilizing agents*) for the different electron-deficient metal ions in coordination chemistry [1, 8]. Among the very wide spectrum of applications (*e.g. the use in photo-converting systems to energy-rich compounds or to electricity* [9–12]), these synthesized coordination complexes based on pyridines have been extensively employed in photochemical sensation [13–16]. Therefore, they have long been considered the benchmark for understanding many of the photochemical properties of transition metal complexes [1, 17].

Elsewhere in literature [18–22] it has been shown that structural modification of pyridine or pyridine derivatives practices a pronounced effect on photochemistry and dynamics of related complexes. Where, the presence of nitrogen atom in the ligation sphere of the pyridine chelating center, dramatically alters the energy mapping of the HOMO-LUMO (*highest occupied molecular orbital-lowest unoccupied molecular orbital*) and therefore, the energy of the lowest energy intra-ligand charge transfer transitions [13–16, 23].

As such, studying pyridine and/substituted pyridines has attracted the attention of researchers. Where how far, substituent modification (*in terms of number, type, or location of substituent(s)*) on pyridine ring exerts changes on either the close or the more distant neighborhoods of pyridyl-N atom and consequently to what extent this modification has reflected on basicity (*the nitrogen two 2p-type electrons*) of pyridine is chiefly discussed in this chapter.

In one of the related publications [15] coordination complexes of the type: $[\text{Ru}(\text{en})_2\text{L}_2]_2$, en = ethylenediamine, L = pyridine or substituted pyridine, namely, methyl-, acetyl-, and cyanopyridine, have been theoretically studied. Results indicated that, changing either the type or position of the substituent(s) placed on the coordinated pyridine chelate could facilitate transitions to appear in the visible region. Interestingly, this enables furnishing of colorimetric chemosensors based on the motivated chemo-luminescence properties of the synthesized metal-pyridine inorganic coordination compounds.

Herein, in the following sections, we will introduce some examples that have been discussed in the reported investigations and how the findings in these studies had led to enrich the thorough understanding of how pyridine structure may interrelate to the dynamics of electronic delocalization over pyridine ring and how this, at the end, would recruit modifications in the optical properties of the investigated pyridine derivatives.

In the first study [24] pyridine, $\text{C}_5\text{H}_5\text{N}$, and pyridine simulations of the type $\text{C}_5(\text{X})_n\text{H}_{5-n}\text{N}$ ($\text{X} = -\text{C} \equiv \text{C}-\text{H}$; $-\text{C} \equiv \text{C}-\text{F}$; $-\text{C} \equiv \text{N}$; $-\text{CH}(\text{=O})$) were theoretically studied employing density functional theory (DFT) and time-dependent density functional theory (TDDFT) calculations at the B3LYP/LANL2DZ level of theory.

Gathered results have indicated that substituent type, number, and position had interestingly affected the charge density localization/delocalization on pyridyl nitrogen of the investigated pyridine simulates. For example, substituted pyridine simulates were shown to possess higher stabilization energy compared to that of unsubstituted pyridines. In addition, and regarding the effect of the number of substituents positioned on pyridine ring, more stability was gained when the number of substituents on the ring was increased. For instance,

ortho-, *meta*-, *para*-trisubstituted C_5H_5N simulate with $-C \equiv C-H$ substituent; abbreviated as $C_5H_2N(o,m,p-C \equiv CH)_3$ was having greater optimum energy (-476.6 a.u) than the *ortho*, *ortho*-disubstituted ($C_5H_3N(o,o-C \equiv CH)_2$, optimum energy = -400.5 a.u) or *ortho*-monosubstituted ($C_5H_4N(o-C \equiv CH)$, optimum energy = -324.4 a.u). This is of course, compared to the unsubstituted pyridine simulate C_5H_5N (optimum energy = -248.2 a.u), see **Table 1** and **Figure 1**.

Looking at **Table 1**, one can easily observe the followings:

- Regardless of the substituent number, the optimum energy of pyridine simulates increases as the number of substituents on the simulate increases. For example, the highest optimum energy is recorded for the pentasubstituted ones **Table 1**.
- Excluding the substituent number, the effect of substituent type is clearly seen when the substituent $-C \equiv C-H$ was replaced by either $-C \equiv N$ or $-C \equiv C-F$ substituents, where increasing the optimum energy follows the order $-C \equiv C-H < -C \equiv N < -C \equiv CF$. For example, compare ($C_5H_2N(o,m,p-C \equiv CH)_3$, -476.6 a.u) with ($C_5H_2N(o,m,p-C \equiv N)_3$, -524.9 a.u) and ($C_5H_2N(o,m,p-C \equiv CF)_3$, -774.3 a.u).

The observed enhancement in stabilization energy of the pyridine as a result of changing the substituent type is believed to be related to the type of the atom tethered to the tail of the carbon-carbon; $-C \equiv C$ triple bond (*these are: N-atom in $-C \equiv N$ substituent and F-atom in $-C \equiv C-F$ substituent*). In result, this indicates that pyridine is very responsive to even slight changes in the structure of the substituent.

Compound	Optimum energy (a.u)	APT-charge on pyridyl nitrogen (a.u)	Average bond length of <i>ortho</i> C=N
C_5H_5N	-248.2	-0.337	1.35828
$C_5H_4N(o-C \equiv CH)$	-324.4	-0.346	1.36738
$C_5H_3N(o,o-C \equiv CH)_2$	-400.5	-0.372	1.36326
$C_5H_2N(o,m,p-C \equiv CH)_3$	-476.6	-0.411	1.36372
$C_5N(o,o,m,p,p-C \equiv CH)_5$	-628.9	-0.411	1.35747
$C_5H_4N(o-C \equiv N)$	-340.5	-0.302	1.36253
$C_5H_3N(o,o-C \equiv N)_2$	-432.7	-0.285	1.35783
$C_5H_2N(o,m,p-C \equiv N)_3$	-524.9	-0.289	1.35789
$C_5N(o,o,m,p,p-C \equiv N)_5$	-709.3	-0.346	1.35245
$C_5H_4N(o-C \equiv CF)$	-423.6	-0.356	1.36598
$C_5H_3N(o,o-C \equiv CF)_2$	-599.0	-0.396	1.36233
$C_5H_2N(o,m,p-C \equiv CF)_3$	-774.3	-0.427	1.36276
$C_5N(o,o,m,p,p-C \equiv CF)_5$	-1125.0	-0.438	1.35648

Table 1. Optimum energy, APT partial charge of pyridyl nitrogen atom and bond length of *ortho* C=N bond in the substituted pyridines compared to that in unsubstituted parent pyridine.

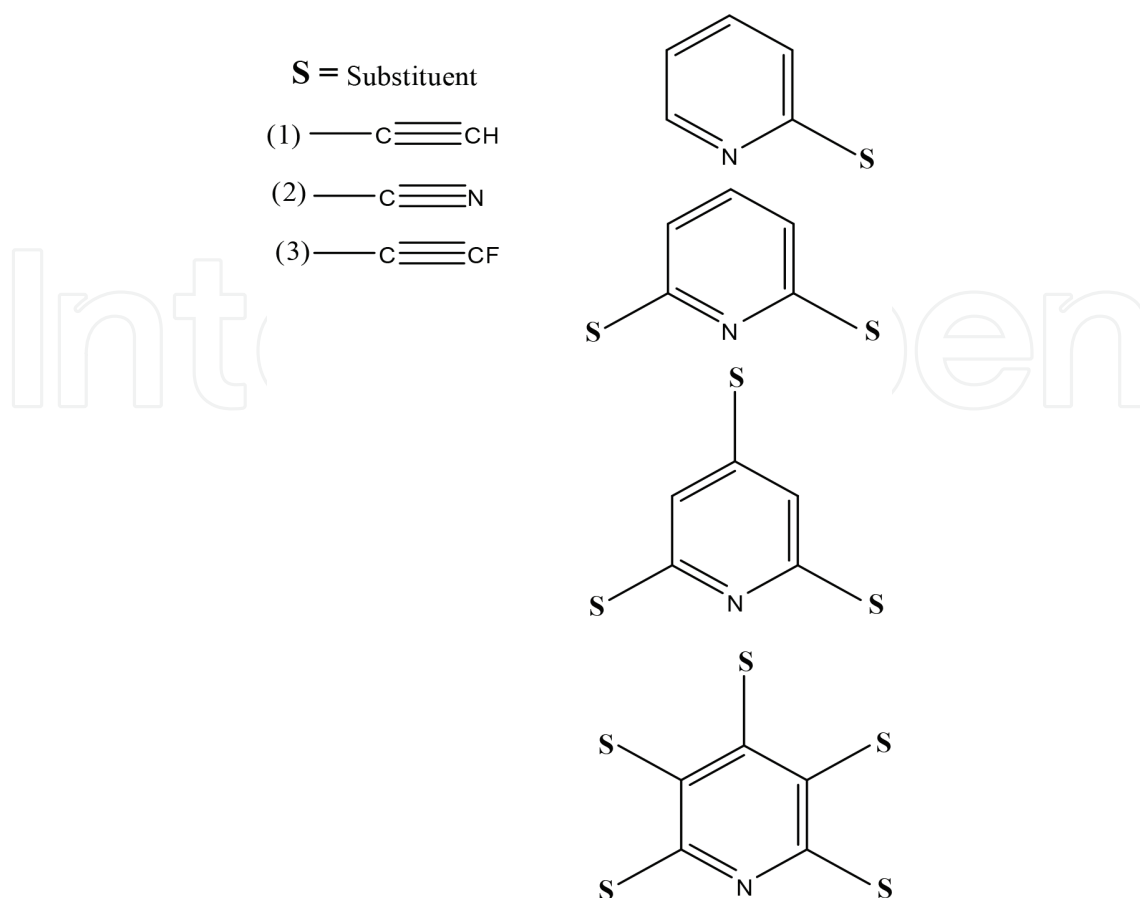


Figure 1. Schematic structures of substituted pyridine simulatates, showing the position, number and type of some substituents placed on the ring of the simulated pyridine.

- c. Calculating the APT-charge (The Atomic Polar Tensor approach [25, 26]) on pyridyl nitrogen was utilized to monitor the changes in electron density enrichment of pyridyl nitrogen as a result of substituent modification, **Figure 4**. This was very important and beneficial, by being helpful in exploring the effectiveness of pyridyl nitrogen toward binding the targeted electron-deficient metal ion.

Actually calculation results of APT-charge on atoms have shown that various substituents tend to affect the charge density accumulation on pyridyl nitrogen differently. The meant electron density localization/delocalization was inherently found to be highly dependent on the type, number, and position of the substituent(s) attached to the simulate. For instance, $\text{—C}\equiv\text{C—F}$ compared to $\text{—C}\equiv\text{C—H}$ and $\text{—C}\equiv\text{N}$ was found to enrich (*or concentrates*) the charge density on pyridyl nitrogen the most. This, as pointed ahead, was attributed to the existence of the fluorine atom at the tail of the attached $\text{—C}\equiv\text{C—F}$ substituent. The fluorine atom, through its own p-orbitals, was capable of expanding the electron density delocalization pathway more compared to that of the two substituents; $\text{—C}\equiv\text{C—H}$ and $\text{—C}\equiv\text{N}$, **Table 1** and **Figure 4**.

From the other side, and from coordination chemistry point of view, studying charge density accumulation employing pyridine simulatates is essential especially when it is

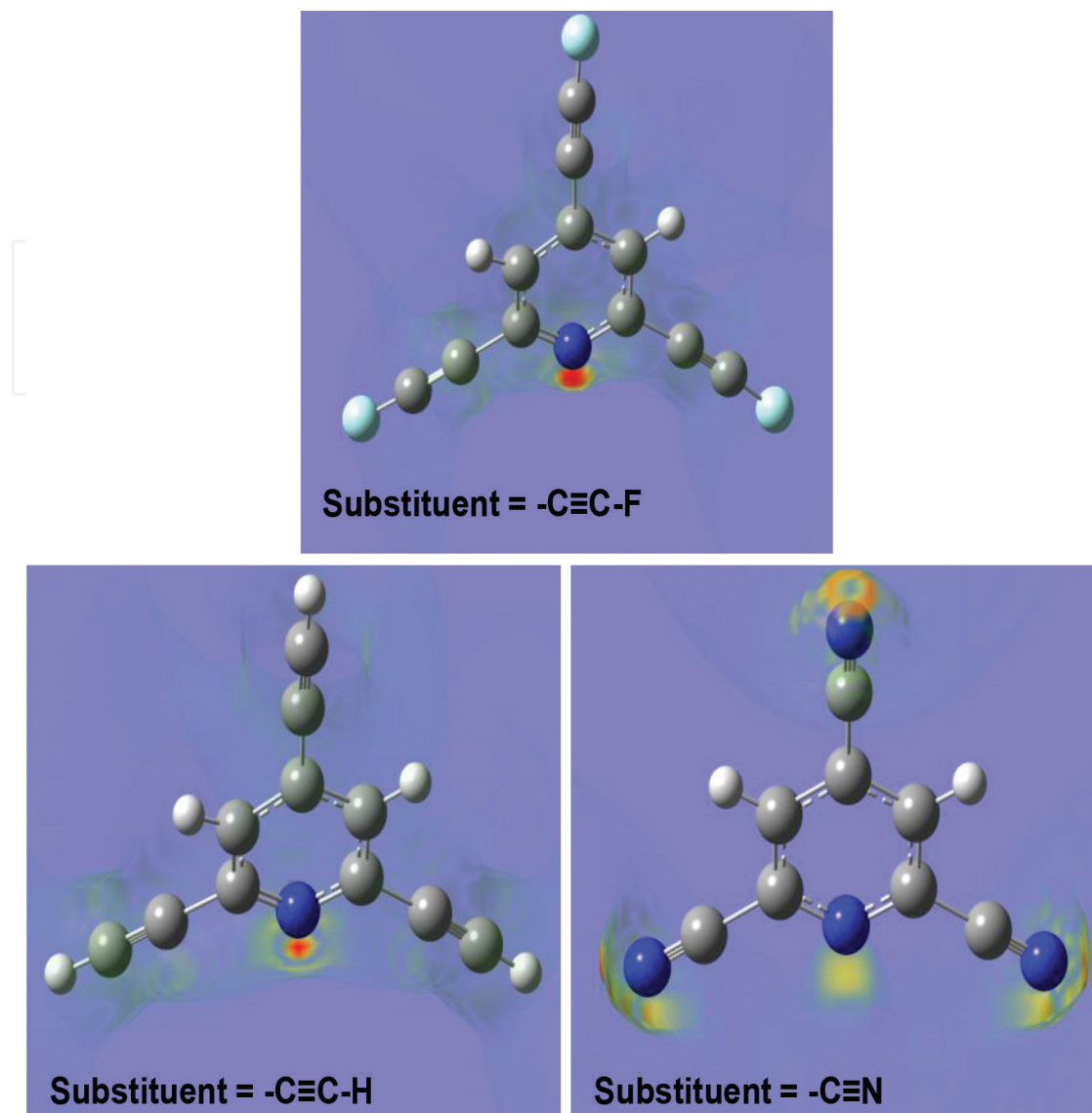


Figure 2. Images of APT-charge distribution of pyridine trisubstituted simulates, showing the variation in charge density on N-atom depending on substituent type. The charge density on N-atom is represented by the intense red-colored spot.

attempted to draw the map of the charge density distribution over atoms constituting the pyridine ring system in general and over pyridyl nitrogen atom in particular. In addition, it also shows how substituent modification interferes with the nitrogen donation capability (*whether reinforced or weakened*) as a result of either dispersing or accumulating the charge density on the nitrogen atom itself or on the other atoms in the close proximity of nitrogen, **Figure 2**.

- d. In the referred study, it was reasonable to relate the amount of APT-charge on pyridyl nitrogen to the bond length of the ortho-C=N bond. The key in establishing this relationship between the two is based on the fact that passage of electrons through a given bond affects its force constant. This in effect appears as a change in bond distance of the given bond.

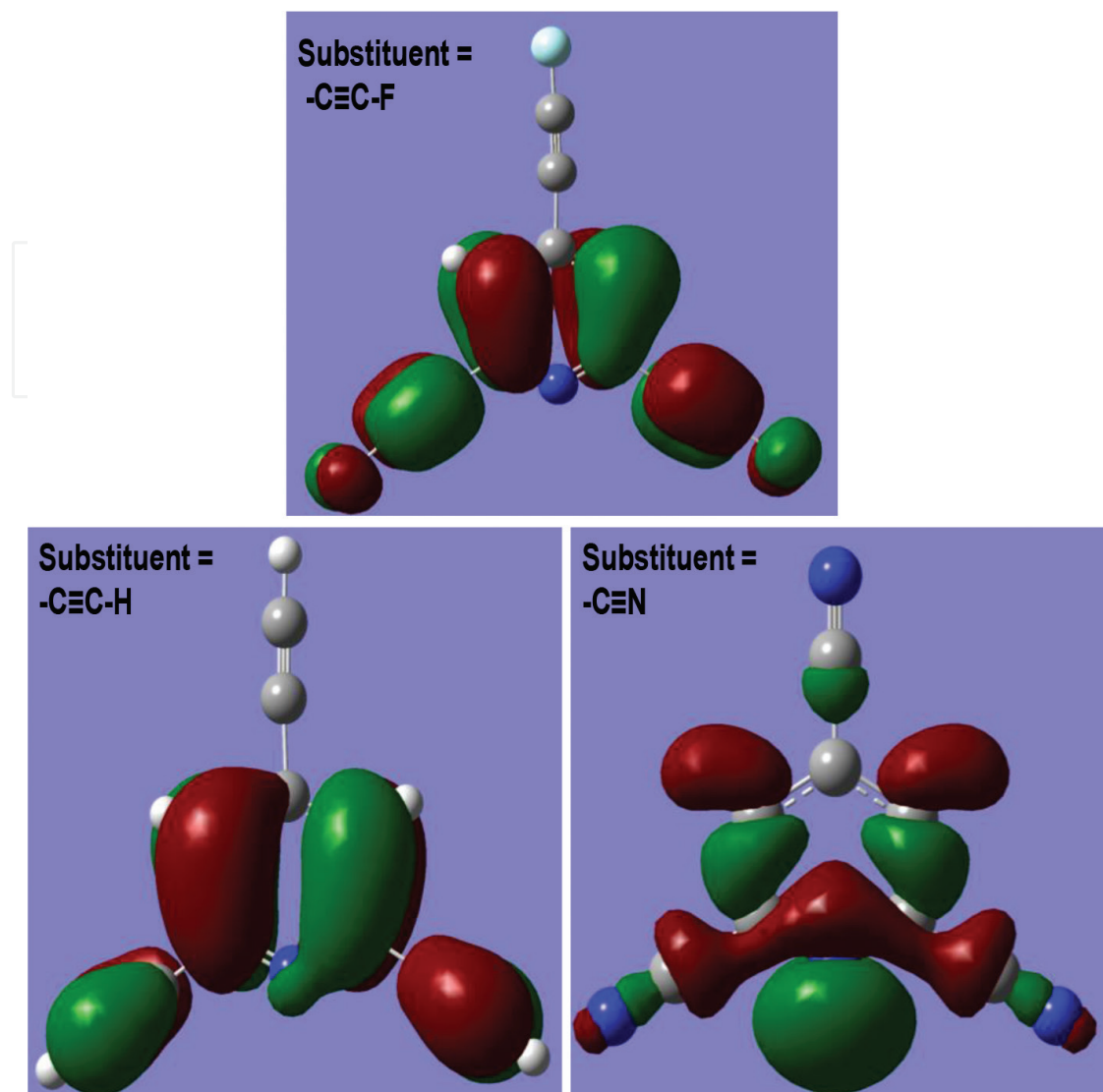


Figure 3. Images of the frontier HOMO molecular orbital component of pyridine trisubstituted simulates, showing the occupation depending on substituent type.

Correlating the values of the *ortho*-C=N bond length with the charge density accumulated on pyridyl nitrogen (see **Table 1**) supports the fact that substituent modification does affect the bond length of the *ortho*-C=N bond in consequence to changing the amount of charge density on pyridyl nitrogen.

Thus, bond length calculations were actually employed to track the variation in charge density in the vicinity of pyridyl nitrogen as a function of substituent modification (**Figure 3**). Why this is important, since it provides deep insights of how charge density is distributed around the pyridyl nitrogen and therefore, how the substituent modification drives nitrogen to be stronger or weaker donor.

Going back to the data presented in **Table 1**, we find that, trisubstituted simulate $\text{C}_5\text{H}_2\text{N}(o,m,p-\text{C}\equiv\text{CH})_3$ of charge density -0.411 a.u and 1.36372 Å⁰ bond length shows smaller charge density value and larger bond length relative to the trisubstituted simulate $\text{C}_5\text{H}_2\text{N}(o,m,p-\text{C}\equiv\text{CF})_3$ which has a charge density of -0.427 and 1.36276 Å⁰ bond length.

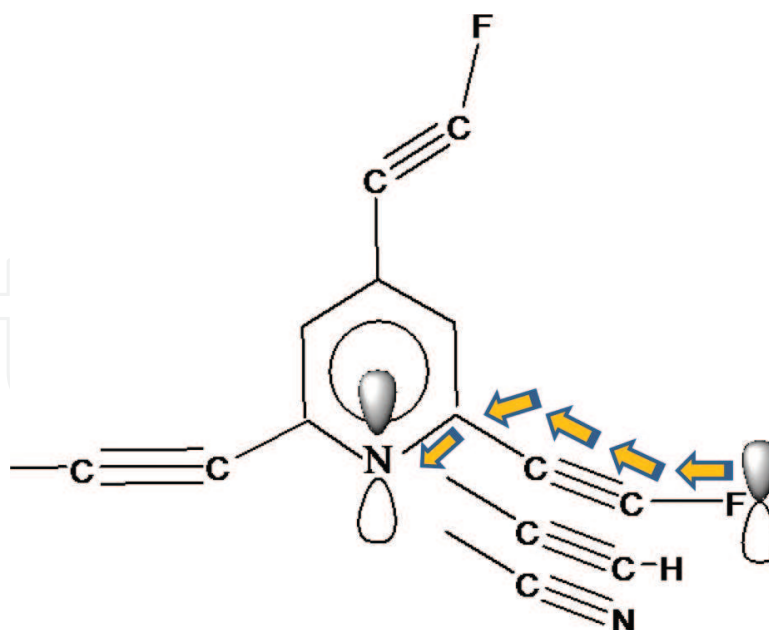


Figure 4. Oversimplified plot showing the assumed extension in the electronic density delocalization pathway generated by the p-orbitals of the fluorine atom on $-C\equiv C-$ substituent compared to H or N-atoms.

From the proceeding, it is obvious that, the most interesting outcomes of the referred study are that, various substituents tend to affect the charge density localization/delocalization differently and found to be highly dependent on the type, number, and position of the substituent attached to the simulate.

Among the investigated substituents ($-C\equiv C-H$, $-C\equiv C-F$, $-C\equiv N$) the substituent $-C\equiv C-F$ was found to be the most efficient in enriching the charge density on pyridyl nitrogen. The fluorine atom [24, 27] existed at the end of the substituent was held responsible for this uniqueness in improving the basicity (*and thus the donating effectiveness*) of the pyridine ring as a whole and pyridyl nitrogen in specific, this is relative to the other two substituents. In effect, the nitrogen atom of the pyridine simulates holding $-C\equiv C-F$ substituent is the one which is promoted the most to act as the efficient stabilizer for the incoming metal ion during coordination process.

Later, and based on the aforementioned findings, one can raise the question: what would be the case if the fluorine atom in $-C\equiv C-F$ substituent is replaced by any other member of the halogen family and how this would affect the basicity of the pyridyl nitrogen. The answer of this questioning came from the outcomes of the study [27] in which calculations on simulates of the type $C_5(S)_n H_{5-n} N$ ($S = -C\equiv C-X$, $X = F, Cl, Br, I$) were conducted.

As it was the case in the studies presented ahead, substituents built up from halogenated carbon-carbon triple bond were introduced onto the pyridine ring in many different forms, for examples some of them were based on monosubstitution at the *ortho*-position and others were introduced onto the pyridyl ring in the form of multisubstituents (*di*-, *tri*- and *penta*-fashions), **Figure 1**.

Responses for substituent modification were monitored by calculating the APT-charge density on nitrogen along with the bond length of the neighboring *ortho* carbon-nitrogen double bond [15, 24, 28–31]. In addition, the distribution of charge density within the simulated system was explored by generating the APT-charge distribution surfaces and the HOMO-molecular orbitals.

Effect of substituent halogenation on electron density enrichment of the pyridine nitrogen, and thus its effectiveness as an electron donor have been investigated. Computational results showed that, substituent halogenation does affect the charge density accumulation on the nitrogen atom of pyridine as well as the $C_2 = N$ bond length, **Table 2**. In addition, the most interesting finding was that charge density localization on pyridyl nitrogen atom has been found to depend on the type of halogen tethered to the triple bond of the attached substituent, this is among other factors. Hardness of the halogen atom attached to the tail of the attached substituent also has been proved to be the determining factor in promoting and qualifying the substituted pyridine to act as an effective electron donor.

The values of the APT-charge on nitrogen were found to increase depending on the substituent order: $-C \equiv C-F < -C \equiv C-Cl < -C \equiv C-Br < -C \equiv C-I$, which is basically the same order of decreasing the hardness of halogens. The maximum enrichment of charge density around nitrogen atom was observed for the iodated triply bonded carbon-carbon substituted pyridines, **Table 2** and **Figure 5**.

Compound	APT-charge on pyridyl nitrogen (a.u)	Bond length of <i>ortho</i> C=N (Å ⁰)
C ₅ H ₅ N	-0.337	1.35828
C ₅ H ₄ N(<i>o</i> -C≡C—F)	-0.356	1.36598
C ₅ H ₄ N(<i>o,o</i> -C≡C—F) ₂	-0.396	1.36233
C ₅ H ₄ N(<i>o,m,p</i> -C≡C—F) ₃	-0.438	1.36276
C ₅ H ₄ N(<i>o,o,m,p,p</i> -C≡C—F) ₅	-0.427	1.35648
C ₅ H ₄ N(<i>o</i> -C≡C—Cl)	-0.365	1.36691
C ₅ H ₄ N(<i>o,o</i> -C≡C—Cl) ₂	-0.419	1.36296
C ₅ H ₄ N(<i>o,m,p</i> -C≡C—Cl) ₃	-0.476	1.36349
C ₅ H ₄ N(<i>o,o,m,p,p</i> -C≡C—Cl) ₅	-0.469	1.35714
C ₅ H ₄ N(<i>o</i> -C≡C—Br)	-0.372	1.36732
C ₅ H ₄ N(<i>o,o</i> -C≡C—Br) ₂	-0.436	1.36315
C ₅ H ₄ N(<i>o,m,p</i> -C≡C—Br) ₃	-0.502	1.36384
C ₅ H ₄ N(<i>o,o,m,p,p</i> -C≡C—Br) ₅	-0.493	1.35751
C ₅ H ₄ N(<i>o</i> -C≡C—I)	-0.380	1.36752
C ₅ H ₄ N(<i>o,o</i> -C≡C—I) ₂	-0.454	1.36351
C ₅ H ₄ N(<i>o,m,p</i> -C≡C—I) ₃	-0.530	1.36411
C ₅ H ₄ N(<i>o,o,m,p,p</i> -C≡C—I) ₅	-0.519	1.35778

Table 2. APT partial charge of pyridyl nitrogen atom and bond length of *ortho* C=N bond in the halogenated triply-C≡C-bonded substituted pyridines compared to that in unsubstituted parent pyridine.

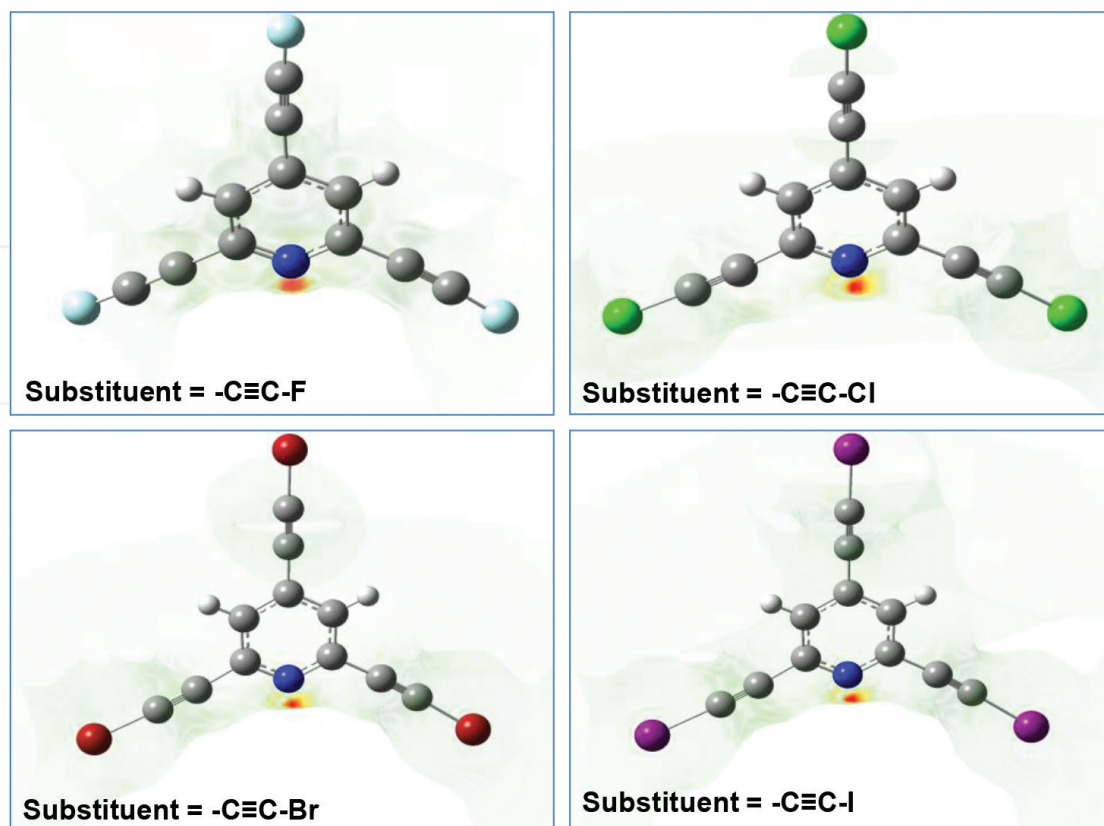


Figure 5. Images of APT-charge distribution of halogenated triply $-\text{C}\equiv\text{C}-$ bonded trisubstituted pyridines, showing the variation in charge density on N-atom depending on substituent type.

The conclusions extracted from the referred [27] study support the proceeded findings of the earlier studies [15, 24], where deeper insights on the key factors that may qualify chelates to function as good stabilizers for metal ions in coordination complexes were gained. This of course is very valuable since it is highly demanded in the field of chemosensation.

As seen in **Table 2**, and in contrast to other analogs, the iodated trisubstituted simulates show the highest accumulation of electron density around nitrogen, indicating that much higher charge density was accumulated on nitrogen by iodine (*the softest halogen*) being tethered at the tail of the carbon-carbon triple bond of the substituent on pyridine. This is compared to the other members of halogens.

In the section of final conclusions drawn in the aforementioned study, the hardness of halogen atom attached to the tail of the substituent undoubtedly was held responsible for controlling the amount of charge density localized on the nitrogen atom of the simulate. This amount of charge density on nitrogen increases as halogen atom changes in the order F, Cl, Br and I, **Table 2**.

In this investigation, it was quite interesting to witness the halogen atom (*which is tethered to the triple bond at the far end of the substituent on pyridine*) masters the donation effectiveness of the pyridyl nitrogen and thus may promote or prohibit the tendency of the pyridine chelate to act as an efficient stabilizer for the targeted electron-deficient metal ion. Wise investing of this property in

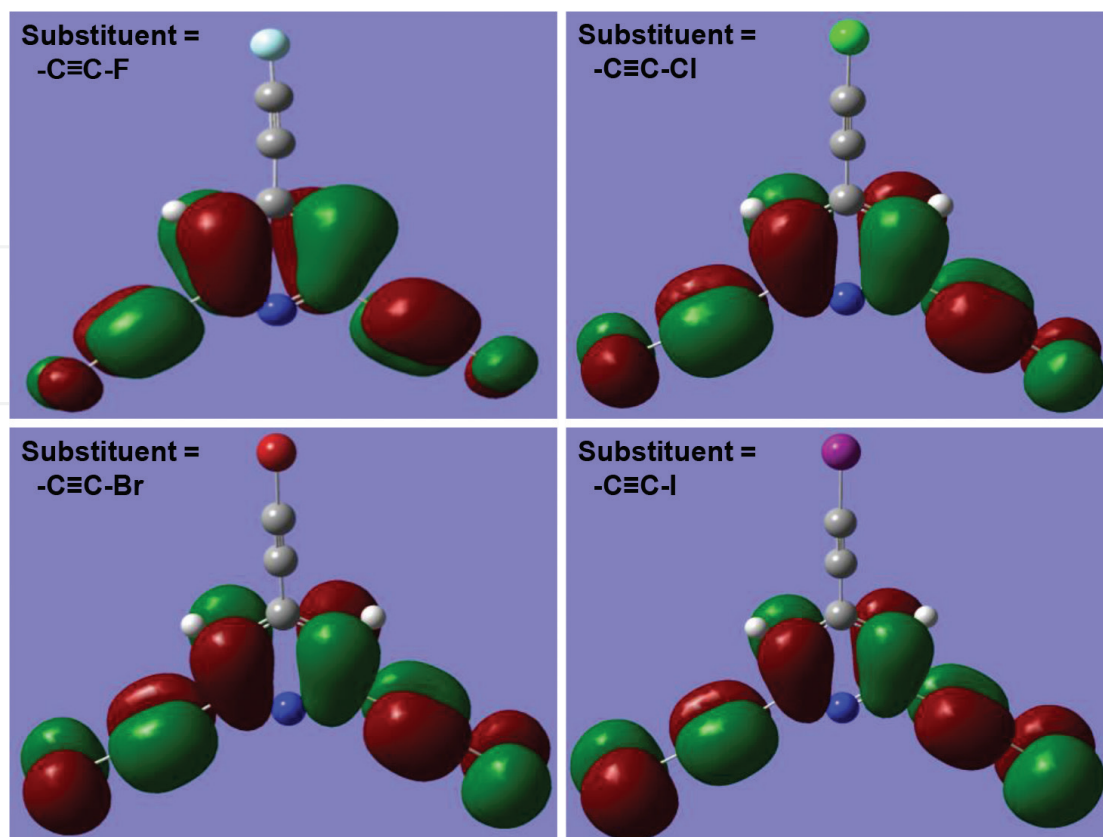


Figure 6. Images of the frontier HOMO molecular orbital component of halogenated triply $-C\equiv C-$ bonded trisubstituted pyridines, showing the occupation depending on the substituent type.

analogous systems would enable synthesizing new generations of pyridine derivatives that are hopefully suitable for engineering a low-energy absorbers, the type of inorganic coordination complexes that are essential and highly demanded in the field of colorimetric chemosensation.

Changes in bond distance of the $C_2 = N$ bond were relied on as extra supporter for the suggested migration image of charge density toward halogen and away from nitrogen, **Table 2**.

This was acceptable, since any variation in the charge density localization on nitrogen would be accompanied by a direct reflection on the $C_2 = N$ bond length. This is equivalent to say that, the more the charge density is localized on nitrogen atom, the less the charge density is swept away from nitrogen or passed through the $C_2 = N$ bond, meaning that weaker (*smaller force constant*) bond will be. For example, trisubstituted simulates (*which have recorded the highest values of charge density enrichment on nitrogen*) are found to exhibit $C_2 = N$ bond lengthening compared to free pyridine, **Table 2**. In other words, this means that, introduction of the halogenated substituent(s) in the form of trisubstitution described in **Figure 1** has led the charge density to accumulate on nitrogen and therefore effectively improved the donation capability of pyridyl nitrogen.

Looking at the shapes of HOMOs (*highest occupied molecular orbitals*) shown in **Figure 6** enables mapping the charge density distribution on atoms of the pyridine moiety.

As seen in the figure, the HOMO of the simulate bearing the $-C\equiv C-F$ substituent extends over the C_2-C_3 , C_5-C_6 atoms including nitrogen and the loops are notably larger in size compared to

that observed for the other simulates which are based on Cl-, Br- and I-halogenated substituents. The HOMO loops were reduced in size as the halogen atom changes in the order F, Cl, Br and I, indicating the dependence of the HOMO expansion on the hardness of the halogen atom attached to the substituent. Noticeably, as more charge density is withdrawn from pyridyl nitrogen toward halogen, larger-sized HOMO loops are anticipated, for example compare $-C \equiv C-F$ simulate with $-C \equiv C-I$ simulate, **Figure 6**.

The same argument is applied, when the APT-charge density is correlated to the absorption energy of the simulate. In the same study, it has been pointed that, as more charge density is localized on nitrogen, a pronounced red shift in the absorption energy of the simulate is observed. This reveals that HOMO/LUMO molecular orbitals practice a narrow energy gap, and therefore simulates of higher APT-charge density on nitrogen are expected to show longer wavelength energy bands of absorption. This finding is considered as the most interesting and advantageous finding in the referred study, where it suggests the possibility of controlling the absorption energy of a particular simulate by playing with the hardness of the halogen atom attached to the tail of the attached substituent(s) on pyridines.

2. Conclusions

The overall conclusion that can be deduced from the aforementioned review is that various substituents can exert pronounced and beneficial effects on charge density enrichment of the pyridyl nitrogen atom in pyridines.

This in result allows stating that substituent modification (*in the form of number, type or position of substitution*) can be employed as a tool for controlling the donation effectiveness of the nitrogen atom in pyridines.

These achievements are essential, when inorganic complexes are demanded to be utilized in the field of chemosensation to feasibly engineer low-energy optically active luminescent inorganic compounds.

Conflict of interest

The author declares that he has no conflict of interest regarding publication of this chapter.

Author details

Amer A. G. Al Abdel Hamid

Address all correspondence to: amerj@yu.edu.jo

Department of Chemistry, Yarmouk University, Irbid, Jordan

References

- [1] Krygowski TM, Szatyłowicz H, Zachara JE. How H-bonding Modifies Molecular Structure and δ -Electron Delocalization in the Ring of Pyridine/Pyridinium Derivatives Involved in H-Bond Complexation. *The Journal of Organic Chemistry*. 2005;**70**:8859
- [2] Kenneth RA. New Density Functional and Atoms in Molecules Method of Computing Relative pKa Values in Solution. *The Journal of Physical Chemistry. A*. 2002;**106**(49): 11963
- [3] Marcus YJ. The Effectivity of Solvents as Electron Pair Donors. *Solution Chemistry*. 1984; **13**:599
- [4] Huynh M, Hiskey M, Ernest L. Polyazido High-Nitrogen Compounds: Hydrazo- and Azo-1,3,5-triazine. *Angewandte Chemie, International Edition*. 2004;**43**:4924
- [5] Li XT, Pang SP, Luo YJ. New Advances in N-Oxidation of Nitrogen-Containing Heterocyclic Compounds. *Chinese Journal of Organic Chemistry*. 2007;**27**:1050
- [6] Zhou Y, Long XP, Wang X. DFT Studies on the Tetrazine Substituted by Six-membered C–N Heterocyclic Derivatives. *Chinese Journal of Energetic Materials*. 2006;**14**:315
- [7] Liu H, Wang F, Wang G-X, Gong X-D. Theoretical studies of -NH₂ and -NO₂ substituted dipyridines. *Molecular Modeling*. 2012;**18**:4639
- [8] Institute for Scientific Information. Philadelphia (1996-2005); Retrieved June 2005
- [9] Johansson E et al. Spin-Orbit Coupling and Metal-Ligand Interactions in Fe(II), Ru(II), and Os(II) Complexes. *Journal of Physical Chemistry C*. 2010;**114**:10314
- [10] Gratzel M. Photoelectrochemical Cells. *Nature*. 2001;**414**:338 DOI: 10.1038/35104607
- [11] Hagfeldt A, Gratzel. M. Molecular Photovoltaics. *Accounts of Chemical Research*. 2000; **33**:269
- [12] Acevedo JH, Brennaman MK, Meyer T. Chemical Approaches to Artificial Photosynthesis. *Journal of Inorganic Chemistry*. 2005;**44**:6802
- [13] Amer A. Hamid et al. A Selective Optical Chemosensor for Iron(III) Ions in Aqueous Medium Based on [bis(2,2'-bipyridine)-bis(2-carboxypyridine)] ruthenium(II) Complex. *Jordan Journal of Chemistry*. 2011;**6**(4):393
- [14] Amer A. Hamid et al. *International Journal of Inorganic Chemistry* 2011;**2011**:6. Article ID 843051. DOI: 10.1155/2011/843051
- [15] Hamid AA. *Research on Chemical Intermediates*. 2012;**38**(9)
- [16] Hamid AA, Kanan S. *Journal of Coordination Chemistry*. 2012;**65**(3):420
- [17] Seddon KR. Coordination compounds. *Coordination Chemistry Reviews*. 1982;**41**:79
- [18] Juris A et al. *Coordination Chemistry Reviews*. 1988;**84**:85

- [19] Roundhill DM. *Photochemistry and Photophysics of Metal Complexes: Modern Inorganic Chemistry Series*. New York: Plenum Press; 1994
- [20] Kalyanasundaram K. *Photochemistry of Polypyridine and Porphyrin Complexes*. New York: Academic Press; 1992
- [21] Dovletoglou A, Adeyemi SA, Meyer TJ. *Inorganic Chemistry*. 1996;**35**:4120
- [22] Liu Y et al. Ru(II) Complexes of New Tridentate Ligands: Unexpected High Yield of Sensitized O₂. *Inorganic Chemistry*. 2009;**48**:375
- [23] Bryan Sears R, Joyce LE, Turro C. Electronic tuning of Ruthenium complexes with 8-quinolate ligands *Photochemistry and Photobiology*. 2010;**86**:1230
- [24] Hamid A, Kanan S, Tahat ZA. DFT analysis of substituent effects on electron-donating efficacy of pyridine. *Research on Chemical Intermediates*. 2014. DOI: 10.1007/s11164-014-1783-6
- [25] Cioslowski J. A new population analysis based on atomic polar tensors. *Journal of the American Chemical Society*. 1989;**111**:8333
- [26] Gross KC, Seybold PG, Hadad CM. Comparison of different atomic charge schemes for predicting pKa variations in substituted anilines and phenols. *International Journal of Quantum Chemistry*. 2002;**90**:445
- [27] Abdel Hamid A et al. Chemosensor Engineering: Effects of Halogen Attached to Carbon-Carbon Triple Bond Substituent on Absorption energy of Pyridine: DFT-Study. *Jordan Journal of Chemistry*. 2016;**11**(1):8
- [28] Manz TA, Sholl DS. Improved Atoms-in-Molecule Charge Partitioning Functional for Simultaneously Reproducing the Electrostatic Potential and Chemical States in Periodic and Nonperiodic Materials. *Journal of Chemical Theory and Computation*. 2012;**8**(8): 2844
- [29] Dunning TH, Hay PJ. *Modern Theoretical Chemistry*. Schaefer. In: H. F III Ed, editor. New York: Plenum; 1976. 1-28
- [30] Cramer CJ. *Essentials of Computational Chemistry: Theories and Methods*. Wiley; 2002. pp. 278-289
- [31] Heinz H, Suter UW. Atomic Charges for Classical Simulations of Polar Systems. *The Journal of Physical Chemistry. B*. 2004;**108**:18341

